International Journal of Development Mathematics Vol 1 Issue 1 Page No. 165 - 183

INTERNATIONAL JOURNAL OF DEVELOPMENT MATHEMATICS

ISSN: 3026-8656 (Print) | 3026-8699 (Online)

journal homepage: https://ijdm.org.ng/index.php/Journals

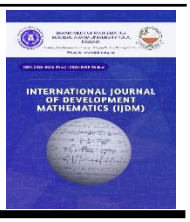

Mathematical Modelling of COVID-19 with Vaccination, Quarantine and Non-Pharmaceutical Interventions

Abdulrahman Mustapha[a*], Samuel Musa[a], Musa Abdullahi[a] and Abdulmumini Husseini[b].

[a]*Department of Mathematics, Modibbo Adama University, P.M.B 2076 Yola, Adamawa State, Nigeria*

[b]*Department of Mathematics, Nigerian Army University Biu, P.M.B 1500 Biu, Borno State, Nigeria.*

ARTICLE INFO

Article history:
Received 01 January 2024
Received in revised form 27 February 2024
Accepted 03 March 2024

Keywords:
COVID-19, Non-pharmaceutical intervention, Quarantine, Stability analysis, Vaccination

MSC 2020 Subject classification:
34A12, 65L05, 65Z05

ABSTRACT

This study formulated and analyzed a deterministic mathematical model of ten compartments for the transmission dynamics of COVID-19 infection using a system of non-linear ordinary differential equations. The system has disease-free and endemic equilibrium points. The basic reproduction number was obtained using the next-generation matrix method and the stability of the equilibrium points were analyzed. From the qualitative analysis, the disease-free equilibrium point is both locally and globally asymptotically stable. Finally, numerical simulations of the model were carried out using MATLAB R2021a. Based on the result obtained, it was concluded that the implementation of vaccination, non-pharmaceutical intervention as well as contact tracing and quarantine can lead to effective control or elimination of the COVID-19 pandemic. And hence, we recommend that the responsible agencies should create a way of enlightening the public on the need of being vaccinated for COVID-19 so as to prevent themselves from getting infected; also, adequate and effective implementation of vaccination and non-pharmaceutical interventions is required in order to prevent or curtail the COVID-19 infection completely.

1. Introduction

The initial reports of the novel severe acute respiratory syndrome coronavirus 2 (SARS-CoV-2) outbreak that resulted in Corona Virus Disease 2019 (COVID-19) were made in Wuhan, Hubei Province, China in December 2019. (Eric *et al.*, (2020); Pedro *et al.*, (2020); Wu *et al*., (2020)). The COVID-19 simply referred to as coronavirus disease 2019 (WHO, 2020). Comparing it to the outbreaks of the Middle East Respiratory Syndrome (MERS) in 2012 and the severe acute respiratory syndrome (SARS) in 2003, it has a lower death rate but a higher rate of infectivity (Imai *et al*., 2020). Exposure to infected individuals' droplets when coughing or sneezing is recognized to be the way it spreads (Harvard Medical School, 2020).

According to Feng *et al*. (2020), COVID-19 can be highly contagious and spread quickly from person to person. The illness, which is currently a global pandemic, has spread quickly throughout the world, posing serious risks to public health and triggering an economic crisis (Bubar *et al.*, (2021); Pedro *et al.*, (2020); Wu *et al*., (2020)). It has had a significant effect on populations and economies, adding to the strain on health systems globally (Iboi *et al*., (2020), Prieto and Gonzalez, (2021); WHO (2020)). In fact, the COVID-19 pandemic has caused significant disruptions at every socioeconomic level of society (Prieto and Gonzalez, 2021).

Global economy has been disrupted by the COVID-19 pandemic, forcing several nations to reassess their economic objectives (Iboi *et al*., (2020); Madubueze *et al*., (2020)). To stop the spread of COVID-19, the governments of several nations adopted various control measures advised by the WHO, including lockdown, quarantine, isolation, social distance, and movement restrictions (Okuonghae & Omane, 2020; WHO, 2019). Unfortunately, a number of countries have experienced economic downturns, increased rates of crime, lawlessness, inflation, mortality and morbidity, and hunger as a result of these control measures (Okuonghae & Omane, 2020; Ibrahim & Ekundayo, 2020). Nigeria recorded her first case on February 27th, 2020, from an Italian immigrant. Approximately 252,853 confirmed cases, 21,315 active cases, 228,404 discharges, and 3,134 deaths were reported as of January 28, 2022 (NCDC, 2020). Although Nigeria's government has taken steps to stop the COVID-19 virus from spreading, as recommended by the WHO, the country continues to report shockingly high numbers of new cases every day. The daily increase in new cases has been ascribed to either stakeholder error or the control measures' incompatibility with the socioeconomic context of Nigeria (Ibrahim & Ekundayo, 2020; Okuonghae & Omane, 2020).

*Corresponding author. Tel.: +2347068886836
E-mail addresses: Abdulmusty61@gmail.com (Abdulrahman Mustapha).
https://doi.org/10.62054/ijdm/0101.12

For instance, the implementation of complete or partial lockdowns and shutdowns of the economy across the country, particularly in Lagos State (the most populous and industrialized state), Abuja, the Federal Capital Territory (the nation's administrative capital), Kano, the commercial hub of Northern Nigeria, and Ogun State (an additional industrial state in Southwest Nigeria), with the exception of essential workers (such as food vendors, the media, healthcare providers, law enforcement agencies, etc.), resulted in a sharp decline in the nation's gross domestic product. Other effects include the country's poverty, the strangling of small and medium-sized businesses, an increase in crime as a result of adversity, and inflation as a result of scarce resources. The way the public views the illness is impeding the effort to combat COVID-19 in the nation: many continue to hold the view that the illness does not kill Africans, and others think it is a scam created for the benefit of certain individuals (Ibrahim & Ekundayo, 2020). Many continue to organize or participate in events that have been banned for the public, and many continue to disregard the simple safety measures of wearing face masks, washing their hands under running water, or using hand sanitizers (Ibrahim & Ekundayo, 2020; Iboi *et al*., 2020; Okuonghae & Omane, 2020).

The first thought that comes to mind when an epidemic breaks out is, "How can we, as a community, protect ourselves against the epidemic?" In actuality, preventing the spread of infection among a community's population requires careful adherence to infection control protocols. Transmission of infection can be controlled by the identification and diagnosis of persons who may have encountered an infected person, called contact tracing and through the removal of infective individuals from the general population. Strategies such as contact tracing and isolation are important tools in managing the spread of epidemics like the coronavirus (Ministry of Health Ghana, 2019). Historically, quarantine has been used as an effective basic public health control measure to stop the spread of infectious diseases. It is loosely defined as the temporary removal of individuals suspected of having been exposed to a communicable disease (from their immediate home or the general population) (Diagne *et al.*, 2021). The logistical execution of quarantine as a control technique raises a number of questions, including who should be placed under quarantine and how long, as these have significant socioeconomic and public health implications (Safi & Gumel, 2011).

Mathematical models have been assessed and proven to be one of the reliable and useful tools for suggesting control and mitigation strategies for outbreaks of infectious diseases and pandemics. Especially when it comes to limiting or reducing the pathogenicity of infectious diseases, mathematical models of infectious illnesses offer accurate and valuable guidance for decision-making about public health measures. Furthermore, according to Brauer *et al*. (2020) and Madubueze *et al.* (2020), it can provide guidance on health-related decisions including cost-effectiveness and the best methods for containment and intervention.

2. Model Formulation

A deterministic compartmental modeling approach is used to describe the disease transmission dynamics at time t. The total population $N(t)$ is sub-divided into the following sub-populations: susceptible individuals $S(t)$, vaccinated (first dose) $V_1(t)$, vaccinated (second dose) $V_2(t)$, individuals who adhere to non-pharmaceutical protocols $N_P(t)$, exposed individuals $E(t)$, quarantined individuals $Q(t)$, symptomatic infected individuals $I(t)$, asymptomatic individuals $A(t)$, hospitalized individuals $H(t)$ and recovered individuals $R(t)$. Thus,

$$N(t) = S(t) + V_1(t) + V_2(t) + N_P(t) + E(t) + Q(t) + A(t) + I(t) + H(t) + R(t) \quad (1)$$

Individuals are recruited into the population at a rate Π with a fraction ρ vaccinated and the remaining $(1-\rho)$ susceptible. The susceptible population is increased by $\xi(1-\alpha)$, ℓ, ε_1, ε_2 and η, where $\xi(1-\alpha)$ proportion of quarantined individuals who have not been found infected after being contact-traced, ℓ are individuals who stopped adhering to COVID-19 protocol, ε_1 and ε_2 are those who losses their immunity after first and second dose of vaccination respectively and η are individuals who recovered and become susceptible. The susceptible population is decreased by β_s, φ, ν_1 and μ, where β_s is the force of infection defined as $\beta_s = b\left[(\omega_A A + \omega_I I + \omega_H H)/N\right]$, φ is the rate of adhering to COVID-19 protocol, ν_1 is the rate at which the susceptible population received their first dose of vaccine and μ is the natural death rate. The non-pharmaceutical intervention compartment is increased by φ and decreased by ℓ and μ, where ℓ is the rate at which individual stopped adhering to COVID-19 protocol. The vaccinated (first dose) individuals' compartments increased from susceptible individuals compartment who received their first dose of vaccine at the rate ν_1 and also decreased by $\beta_s(1-\in)$, ν_2 and μ, where $\beta_s(1-\in)$ is the force of infection and ν_2 is the rate at which the vaccinated (first dose) individuals' compartments received their second dose

of the vaccine. The vaccinated (second dose) compartment is increased by v_2 and $\rho\Pi$ and decreased by ε_2 and μ. The transition rates from susceptible and vaccinated population to exposed compartment is given by the force of infection $\beta_s = b\left[(\omega_A A + \omega_I I + \omega_H H)/N\right]$ and $\beta_s(1-\in)$ respectively, and is decreased by θ, $\sigma\psi$ and $\sigma(1-\psi)$, where θ is the contact-tracing rate, $\sigma\psi$ is the proportion of exposed individual who become symptomatic infected and $\sigma(1-\psi)$ is the rate at which the exposed individuals become asymptomatic infected. The quarantined population increased by θ and decreased by $\xi\alpha$, $\xi(1-\alpha)$ and μ, where ξ is the exit rate from the quarantine class while α is the proportion of quarantine individuals who are hospitalized. Asymptomatic population is increased by $\sigma(1-\psi)$ and also decreased by $\lambda(1-\phi)$, $\lambda\phi$ and μ, where λ is the exit rate from the asymptomatic class and ϕ is the proportion of asymptomatic individual who recovered naturally. Symptomatic infected population increased by $\sigma\psi$ and $\lambda(1-\phi)$, and decreased by $\gamma(1-\kappa)$, $\gamma\kappa$ and $\mu+\delta$, where γ is the exit rate from the symptomatic infected individuals and κ is the proportion of symptomatic infected individuals who recovered naturally while δ is death due to disease. Hospitalized individuals increased by $\xi\alpha$ and $\gamma(1-\kappa)$, and is decreased by τ and $\mu+\delta$, where τ is the recovered rate of hospitalized individuals. The recovered population is increased by $\lambda\phi$, $\gamma\kappa$ and τ, and is decreased by η and μ.

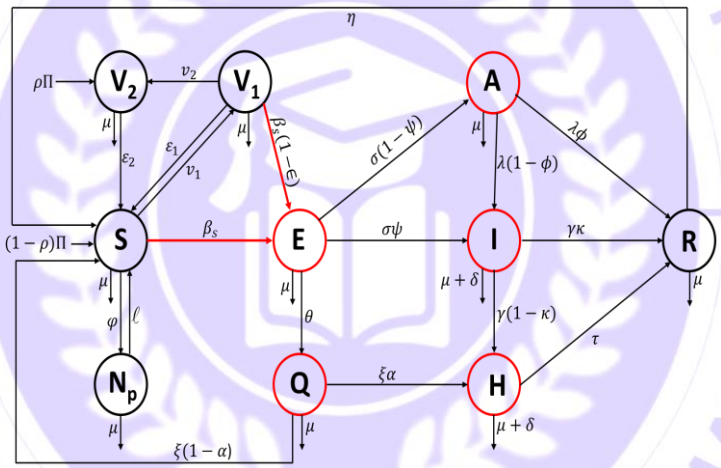

Figure 1: Schematic diagram of the model

Table 1: Description of State Variable used for the study

Variables	Description
$S(t)$	Susceptible population at time t
$V_1(t)$	First dose vaccinated individuals at time t
$V_2(t)$	Second dose vaccinated individuals at time t
$N_p(t)$	Individuals adhering to non-pharmaceutical covid-19 protocols at a time t
$E(t)$	Exposed individuals at time t
$Q(t)$	Quarantined individuals at time t
$I(t)$	Symptomatic infected individuals at time t
$A(t)$	Asymptomatic infected individuals at time t
$H(t)$	Hospitalized individuals under treatments at time t
$R(t)$	Recovered individuals at time t

Table 2: Description of Parameter values used and their source

Parameters	Description	Values	References
Π	Recruitment rate	271	[3]
ρ	Proportion of recruited individuals who are vaccinated	0.0001/day	[7]
ν_1	First dose vaccination rate	0.25, 0.50, 0.75	Assumed
ν_2	Second dose vaccination rate	0.8	Assumed
ε_1	Loss of immunity rate for first dose vaccine	0.010	Assumed
ε_2	Loss of immunity rate for second dose vaccine	0.020	Assumed
ℓ	Rate of non-compliance to covid-19 protocol	0.02	Assumed
φ	Rate at which the susceptible population adhered to covid-19 protocol	0.25, 0.50, 0.75	Assumed
ω_A	Transmission rate by asymptomatic class	0.3	[1]
ω_I	Transmission by symptomatic individuals	1.8	[7]
ω_H	Transmission by hospitalized individuals	0.3	[7]
μ	Natural death rate	0.016	[11]
δ	Disease-induced death rate	0.018	[10]
$\in$	Infection reduction of vaccinated individuals	0.8	[7]
σ	Exit rate from the exposed class	0.13	[23]
γ	Exit rate from the infectious class	0.0833	[2]
κ	Proportion on infectious who recover naturally	0.05	[6]
ψ	Fraction of exposed who become infected	0.7	[1]
b	Effective contact rate	1.12	[2]
τ	Recovery rate of hospitalized individuals	0.0701	[10]
ϕ	Proportion of asymptomatic who recover naturally	0.14	[23]
λ	Exit rate from asymptomatic class	0.13978	[1]
η	Rate at which individuals loss immunity	0.011	[17]
θ	Contact tracing rate for exposed individuals	0.25, 0.50, 0.75	[8]

α	Proportion of individuals in the quarantine class that moved to the treatment class.	0.05	[9]
ξ	Exit rate from the quarantine class	0.06	[8]

From the schematic diagram in Figure 1, we derive the following system of nonlinear ordinary differential equations:

$$\left.\begin{aligned}
\frac{dS}{dt} &= (1-\rho)\Pi + \xi(1-\alpha)Q + \eta R + \ell N_p + \varepsilon_1 V_1 + \varepsilon_2 V_2 - (\beta_s + \nu_1 + \varphi + \mu)S \\
\frac{dN_p}{dt} &= \varphi S - (\ell + \mu)N_p \\
\frac{dV_1}{dt} &= \nu_1 S - [\nu_2 + \varepsilon_1 + \mu + \beta_s(1-\in)]V_1 \\
\frac{dV_2}{dt} &= \rho\Pi + \nu_2 V_1 - (\varepsilon_2 + \mu)V_2 \\
\frac{dE}{dt} &= \beta_S S + \beta_s(1-\in)V_1 - (\sigma + \mu + \theta)E \\
\frac{dQ}{dt} &= \theta E - (\xi + \mu)Q \\
\frac{dA}{dt} &= \sigma(1-\psi)E - (\lambda + \mu)A \\
\frac{dI}{dt} &= \sigma\psi E + \lambda(1-\phi)A - (\gamma + \mu + \delta)I \\
\frac{dH}{dt} &= \xi\alpha Q + \gamma(1-\kappa)I - (\tau + \mu + \delta)H \\
\frac{dR}{dt} &= \lambda\phi A + \gamma\kappa I + \tau H - (\eta + \mu)R
\end{aligned}\right\} \quad (2)$$

with initial conditions

$$S(0) \geq 0, N_p(0) \geq 0, \mathrm{V}_1(0) \geq 0, V_2(0) \geq 0, E(0) \geq 0, Q(0) \geq 0, A(0) \geq 0,\ I(0) \geq 0,$$
$$H(0) \geq 0, \mathrm{R}(0) \geq 0 \quad (3)$$

3. Model Analysis

3.1 Invariant region

To show the boundedness of the solution of the model (2), we have

$$\frac{dN}{dt} = \Pi - \mu\left(\mathrm{S} + \mathrm{V}_1 + \mathrm{V}_2 + \mathrm{N}_p + \mathrm{E} + Q + \mathrm{A} + I + H + R\right) - \delta\left(I + H\right) \quad (4)$$

which gives

$$\frac{dN}{dt} = \Pi - \mu N - \delta(I + H) \quad (5)$$

Therefore, it follows that the biologically feasible region for model (2) is

$$\Omega = \left\{ (S, N_p, V_1, V_2, E, Q, A, I, \mathrm{H}, \mathrm{R}) \in \mathbb{R}_+^{10} : N \le \frac{\Pi}{\mu} \right\} \tag{6}$$

Thus, the closed set Ω is positively invariant.

3.2 Positivity of the model solutions

For the system to be epidemiologically realistic, it is necessary to prove that all the state variables remain positive at all time.

Theorem 1: If $S(0)$, $N_p(0)$, $V_1(0)$, $V_2(0)$, $E(0)$, $Q(0)$, $A(0)$, $I(0)$, $H(0)$, and $R(0)$ are all non-negative, then the solutions $S(t), N_p(t), V_1(t), V_2(t), E(t), Q(t), A(t), I(t), H(t)$, and $R(t)$ are all positive for t ≥ 0.

Proof:

From the system equation (2) we have

$$\frac{dS}{dt} = (1-\rho)\Pi + \xi(1-\alpha)Q + \eta R + \ell N_p + \varepsilon_1 V_1 + \varepsilon_2 V_2 - (\beta_s + \nu_1 + \varphi + \mu)S \tag{7}$$

This can be expressed as

$$\frac{dS}{dt} \ge -(\beta_s + \nu_1 + \varphi + \mu)S \tag{8}$$

Integrating both sides using separation of variables, we have

$$S(t) \ge C_1 \, \mathrm{e}^{-(\beta_s + \nu_1 + \varphi + \mu)t} \tag{9}$$

At time $t = 0$, $S(0) = C_1$. Substituting for C_1 into equation (4.8), we obtained

$$S(t) \ge S(0)\, \mathrm{e}^{-(\beta_s + \nu_1 + \varphi + \mu)\,\mathrm{t}} \tag{10}$$

Hence, $S(t) > 0$ (Positive).

Similarly, it has been follows that

$N_p(t) > 0, V_1(t) > 0, V_2(t) > 0, E(t) > 0, Q(t) > 0, A(t) > 0, I(t) > 0, H(t) > 0, R(t) > 0.$

This proves that the solutions of system (2) are positive for all $t \ge 0$.

3.3 ***Disease-free Equilibrium Point of the Model***

The disease-free equilibrium point of the model (2) is given by

$$E_0^* = \left(S^*, N_p{}^*, V_1^*, V_2^*, 0, 0, 0, 0, 0, 0 \right) \tag{11}$$

Where;

$$\left.\begin{aligned} S^* &= \frac{A_1 A_4 \Pi (A_3 A_5 + \varepsilon_2 \rho)}{A_1 A_3 (A_2 A_4 - \ell\varphi) - A_4 (A_3 \varepsilon_1 \nu_1 + \varepsilon_2 \nu_1 \nu_2)} \\ N_p{}^* &= \frac{A_1 \Pi \varphi (A_3 A_5 + \varepsilon_2 \rho)}{A_1 A_3 (A_2 A_4 - \ell\varphi) - A_4 (A_3 \varepsilon_1 \nu_1 + \varepsilon_2 \nu_1 \nu_2)} \\ V_1^* &= \frac{A_4 \nu_1 \Pi (A_3 A_5 + \varepsilon_2 \rho)}{A_1 A_3 (A_2 A_4 - \ell\varphi) - A_4 (A_3 \varepsilon_1 \nu_1 + \varepsilon_2 \nu_1 \nu_2)} \\ V_2^* &= \frac{\rho \Pi (A_1 A_2 A_4 - A_1 \ell\varphi - A_4 \varepsilon_1 \nu_1)}{A_1 A_3 (A_2 A_4 - \ell\varphi) - A_4 (A_3 \varepsilon_1 \nu_1 + \varepsilon_2 \nu_1 \nu_2)} \end{aligned}\right\} \tag{12}$$

with

$A_1 = (\nu_2 + \varepsilon_1 + \mu), \quad A_2 = (\nu_1 + \varphi + \mu), \quad A_3 = (\varepsilon_2 + \mu), \; A_4 = (\ell + \mu), \quad \text{and } A_5 = (1-\rho)$

3.4 Endemic equilibrium point

In the case where there is infection in the community,

We let:

$$\left.\begin{array}{l} b_1=(\sigma+\mu+\theta),\quad b_2=(v_2+\varepsilon_1+\mu+\beta_s(1-\in)),\quad b_3=(\gamma+\mu+\delta),\quad b_4=(\tau+\mu+\delta) \\ b_5=(\xi+\mu),\quad b_6=(\lambda+\mu),\quad b_7=(1-\varphi),\quad b_8=\lambda(1-\phi),\quad b_9=\sigma(1-\psi),\ b_{10}=\gamma(1-\kappa) \\ b_{11}=(\ell+\mu),\quad b_{12}=(\varepsilon_2+\mu),\ b_{13}=(\beta_s+v_1+\varphi+\mu),\ b_{14}=(1-\rho),\ b_{15}=\xi(1-\alpha) \end{array}\right\} \quad (13)$$

So that, the endemic equilibrium point is given as:

$$E_1^*=\left(S^{**},N_p{}^{**},V_1^{**},V_2^{**},Q^{**},E^{**},A^{**},I^{**},H^{**},R^{**}\right) \quad (14)$$

where;

$$\left.\begin{array}{l} S^{**}=\dfrac{b_1b_2b_3b_{11}[b_{12}(\eta+b_{14})+\prod\varepsilon_2\rho]}{b_{12}[b_{11}(b_1b_3(b_2b_{13}+\varepsilon_1v_1)+\theta\beta_sb_{15}(1+b_2-\in))-\ell\varphi b_1b_2b_3]+\varepsilon_2b_1b_3b_{11}v_1v_2} \\ N_p{}^{**}=\dfrac{\varphi b_1b_2b_3b_{11}[b_{12}(\eta+b_{14})+\prod\varepsilon_2\rho]}{(b_{12}[b_{11}(b_1b_3(b_2b_{13}+\varepsilon_1v_1)+\theta\beta_sb_{15}(1+b_2-\in))-\ell\varphi b_1b_2b_3]+\varepsilon_2b_1b_3b_{11}v_1v_2)(\ell+\mu)} \\ V_1^{**}=\dfrac{v_1b_1b_2b_3b_{11}[b_{12}(\eta+b_{14})+\prod\varepsilon_2\rho]}{\left(b_{12}[b_{11}(b_1b_3(b_2b_{13}+\varepsilon_1v_1)+\theta\beta_sb_{15}(1+b_2-\in))-\ell\varphi b_1b_2b_3]+\varepsilon_2b_1b_3b_{11}v_1v_2\right)\left(v_2+\varepsilon_1+\mu+\beta_s(1-\in)\right)} \\ V_2^{**}=\dfrac{y_1b_1b_2b_3b_{11}[b_{12}(\eta+b_{14})+\prod\varepsilon_2\rho]}{b_{12}[b_{11}(b_1b_3(b_2b_{13}+\varepsilon_1v_1)+\theta\beta_sb_{15}(1+b_2-\in))-\ell\varphi b_1b_2b_3]+\varepsilon_2b_1b_3b_{11}v_1v_2} \\ E^{**}=\dfrac{y_2b_1b_2b_3b_{11}[b_{12}(\eta+b_{14})+\prod\varepsilon_2\rho]}{b_{12}[b_{11}(b_1b_3(b_2b_{13}+\varepsilon_1v_1)+\theta\beta_sb_{15}(1+b_2-\in))-\ell\varphi b_1b_2b_3]+\varepsilon_2b_1b_3b_{11}v_1v_2} \\ Q^{**}=\dfrac{y_3b_1b_2b_3b_{11}[b_{12}(\eta+b_{14})+\prod\varepsilon_2\rho]}{b_{12}[b_{11}(b_1b_3(b_2b_{13}+\varepsilon_1v_1)+\theta\beta_sb_{15}(1+b_2-\in))-\ell\varphi b_1b_2b_3]+\varepsilon_2b_1b_3b_{11}v_1v_2} \\ A^{**}=\dfrac{y_4b_1b_2b_3b_{11}[b_{12}(\eta+b_{14})+\prod\varepsilon_2\rho]}{b_{12}[b_{11}(b_1b_3(b_2b_{13}+\varepsilon_1v_1)+\theta\beta_sb_{15}(1+b_2-\in))-\ell\varphi b_1b_2b_3]+\varepsilon_2b_1b_3b_{11}v_1v_2} \\ I^{**}=\varphi b_6+b_7b_8+\dfrac{\sigma(\beta_sb_2+\beta_s(1-\in)v_1)b_1b_2b_3b_{11}[b_{12}(\eta+b_{14})+\prod\varepsilon_2\rho]b_1b_2b_3b_6}{b_{12}[b_{11}(b_1b_3(b_2b_{13}+\varepsilon_1v_1)+\theta\beta_sb_{15}(1+b_2-\in))-\ell\varphi b_1b_2b_3]+\varepsilon_2b_1b_3b_{11}v_1v_2} \\ H^{**}=\dfrac{\beta_s\left[b_5(\sigma\psi b_6+b_8b_9b_{10}+\xi\alpha\theta b_3b_6\right](b_2+(1-\in)v_1)b_{11}[b_{12}(\eta+b_{14})+\prod\varepsilon_2\rho]}{\left(b_{12}[b_{11}(b_1b_3(b_2b_{13}+\varepsilon_1v_1)+\theta\beta_sb_{15}(1+b_2-\in))-\ell\varphi b_1b_2b_3]+\varepsilon_2b_1b_3b_{11}v_1v_2\right)\left(b_4b_5b_6\right)} \\ R^{**}=\dfrac{1}{b_1b_2b_3b_4b_5b_6(\eta+\mu)}\left(\dfrac{\kappa b_4b_5\gamma(\varphi b_6+b_7b_8)b_1b_2b_3b_{11}(b_{12}(\eta+b_{14})+\Pi\varepsilon_2\rho}{b_{12}(b_{11}(b_1b_3(b_2b_{13}+\varepsilon_1v_1)+\theta\beta_sb_{15}(1+b_2-\in))-\ell\varphi b_1b_2b_3)+\varepsilon_2b_1b_3b_{11}v_1v_2}\right) \end{array}\right\} \quad (15)$$

With

$$\left.\begin{aligned} y_1 &= \frac{\rho\Pi(v_2+\varepsilon_1+\mu+\beta_s(1-\in))+v_2v_1}{(\varepsilon_2+\mu)(v_2+\varepsilon_1+\mu+\beta_s(1-\in))} \\ y_2 &= \frac{[\beta_S(v_2+\varepsilon_1+\mu+\beta_s(1-\in))+\beta_s(1-\in)v_1]}{(\sigma+\mu+\theta)(v_2+\varepsilon_1+\mu+\beta_s(1-\in))} \\ y_3 &= \frac{\theta[\beta_S(v_2+\varepsilon_1+\mu+\beta_s(1-\in))+\beta_s(1-\in)v_1]}{(\xi+\mu)(\sigma+\mu+\theta)(v_2+\varepsilon_1+\mu+\beta_s(1-\in))} \\ y_4 &= \frac{\sigma(1-\psi)[\beta_S(v_2+\varepsilon_1+\mu+\beta_s(1-\in))+\beta_s(1-\in)v_1]}{(\lambda+\mu)(\sigma+\mu+\theta)(v_2+\varepsilon_1+\mu+\beta_s(1-\in))} \end{aligned}\right\} \quad (16)$$

3.5 Basic reproduction number

The basic reproduction number was established using next-generation method (Bubar *et al.*, 2021). The rate of appearance of new infections and the rate of transfer of individuals by all other means are given by the following

$$F=\begin{bmatrix} 0 & \frac{b\omega_I S^*}{N}+\frac{b\omega_I(1-\in)V_1^*}{N} & \frac{b\omega_A S^*}{N}+\frac{b\omega_A(1-\in)V_1^*}{N} & 0 & \frac{b\omega_H S^*}{N}+\frac{b\omega_H(1-\in)V_1^*}{N} \\ 0 & 0 & 0 & 0 & 0 \\ 0 & 0 & 0 & 0 & 0 \\ 0 & 0 & 0 & 0 & 0 \\ 0 & 0 & 0 & 0 & 0 \end{bmatrix} \quad (17)$$

$$V=\begin{bmatrix} (\sigma+\mu+\theta) & 0 & 0 & 0 & 0 \\ -\sigma\psi & (\gamma+\mu+\delta) & 0 & -\lambda(1-\phi) & 0 \\ -\sigma(1-\psi) & 0 & (\lambda+\mu) & 0 & 0 \\ -\theta & 0 & 0 & (\xi+\mu) & 0 \\ 0 & -\gamma(1-\kappa) & 0 & -\xi\alpha & (\tau+\mu+\delta) \end{bmatrix} \quad (18)$$

Thus, the spectral radius $\rho(FV^{-1})$ gives the basic reproduction number of the system (2) as

$$R_0 = \rho(FV^{-1}) = \left\{ \begin{array}{l} \dfrac{-\left(((\rho-1)\mu-\varepsilon_2)b\sigma\mu(\mu+(1-\in)\nu_1+\nu_2+\varepsilon_1)(\ell+\mu)\omega_z(\mu\psi+(-1+\psi)\phi)\lambda\right)}{(\tau+\mu+\theta)(\lambda+\mu)(\mu^4+(\nu_1+\nu_2+\varphi+\varepsilon_1+\varepsilon_2+\ell)\mu^3)+((\ell+\nu_1+\nu_2+\varphi+\varepsilon_1)\varepsilon_2)} \\ +\dfrac{\left(\omega_A b(\mu+(1-\in)\nu_1+\nu_2+\varepsilon_1)((\rho-1)\mu-\varepsilon_2)\mu(\ell+\mu)\sigma(-1-\psi)\right)}{(\tau+\mu+\theta)(\lambda+\mu)\left(((\varepsilon_2+\mu)(\ell+\mu)\varphi+\mu(\mu+\nu_1+\varepsilon_2)\ell+\mu^3+(\nu_1+\varepsilon_2)\mu^2-\ell\varphi\varepsilon_2)\nu_2\right)} \\ +\dfrac{1}{\Pi(\tau+\mu+\theta)(\gamma+\mu+\delta)(\lambda+\mu)(\xi+\mu)(\tau+\mu+\delta)} \\ \left(\dfrac{b\omega_H(\nu_2+\varepsilon_1+\mu)(\ell+\mu)\Pi((\varepsilon_2+\mu)(1-\rho)+\varepsilon_2\rho)}{(\nu_2+\varepsilon_1+\mu)(\varepsilon_2+\mu)((\nu_1+\varphi+\mu)(\ell+\mu)-\ell\varphi-(\ell+\mu)(\varepsilon_2+\mu)\varepsilon_1\nu_1+\varepsilon_2\nu_1\nu_2)}\right) \\ \left(\alpha\theta\xi(\gamma+\mu+\delta)(\lambda+\mu)+\psi\sigma\gamma(1-\kappa)(\lambda+\mu)(\xi+\mu)+\sigma(1-\psi)\gamma(1-\kappa)\lambda(1-\phi)(\xi+\mu)\right) \end{array} \right\} \quad (19)$$

3.6 Local stability of the disease-free equilibrium point

Theorem 2: The Covid–19–free equilibrium points E_0^* of the model equations (2) is stable if $n_i < 0 \ \forall \ i = 1,2,3,\ldots$ of the Jacobian, J evaluated at E_0^*. Where;

$$J = \begin{bmatrix} \dfrac{\partial f_1}{\partial x_1} & \dfrac{\partial f_1}{\partial x_2} & \cdots & \dfrac{\partial f_1}{\partial x_n} \\ \dfrac{\partial f_2}{\partial x_1} & \dfrac{\partial f_2}{\partial x_2} & \cdots & \dfrac{\partial f_2}{\partial x_n} \\ \vdots & \vdots & & \vdots \\ \dfrac{\partial f_n}{\partial x_1} & \dfrac{\partial f_n}{\partial x_2} & \cdots & \dfrac{\partial f_n}{\partial x_n} \end{bmatrix} \quad (20)$$

is the Jacobian of the model equations (2) and n an eigenvalue. The Covid-19-free equilibrium point E_0^* is unstable if at least one of the eigenvalues has a positive real part.

Proof:

The Jacobian Matrix J for the system (2) is given by

$$J(E_0^*) = \begin{bmatrix} -x_1 & \ell & \varepsilon_1 & \varepsilon_2 & 0 & x_2 & 0 & 0 & 0 & \eta \\ \varphi & -x_2 & 0 & 0 & 0 & 0 & 0 & 0 & 0 & 0 \\ \nu_1 & 0 & -x_4 & 0 & 0 & 0 & 0 & 0 & 0 & 0 \\ 0 & 0 & \nu_2 & -x_5 & 0 & 0 & 0 & 0 & 0 & 0 \\ 0 & 0 & 0 & 0 & -x_6 & 0 & 0 & 0 & 0 & 0 \\ 0 & 0 & 0 & 0 & \theta & -x_8 & 0 & 0 & 0 & 0 \\ 0 & 0 & 0 & 0 & x_7 & 0 & -x_9 & 0 & 0 & 0 \\ 0 & 0 & 0 & 0 & \sigma\psi & 0 & x_{10} & -x_{11} & 0 & 0 \\ 0 & 0 & 0 & 0 & 0 & \xi\alpha & 0 & x_{12} & -x_{13} & 0 \\ 0 & 0 & 0 & 0 & 0 & 0 & \lambda\phi & \gamma\kappa & \tau & -x_{14} \end{bmatrix} \quad (21)$$

where:

$$x_1=(\nu_1+\varphi+\mu),\quad x_2=\xi(1-\alpha),\quad x_3=(\ell+\mu),\quad x_4=(\nu_2+\varepsilon_1+\mu),\quad x_5=(\varepsilon_2+\mu)$$
$$x_6=(\sigma+\mu+\theta),\quad x_7=\sigma(1-\psi),\quad x_8=(\xi+\mu),\quad x_9=(\lambda+\mu),\quad x_{10}=\lambda(1-\phi)$$
$$x_{11}=(\gamma+\mu+\delta),\quad x_{12}=\gamma(1-\kappa),\quad x_{13}=(\tau+\mu+\delta),\quad x_{14}=(\gamma+\mu)$$

We then reduce the matrix to upper triangular form. The transformed matrix evaluated at E_0^* is given by

$$J(E_0^*)=\begin{pmatrix}
-x_1 & \ell & \varepsilon_1 & \varepsilon_2 & 0 & x_2 & 0 & 0 & 0 & \eta \\
0 & -T_1 & T_2 & T_3 & 0 & T_4 & 0 & 0 & 0 & T_5 \\
0 & 0 & -T_6 & -T_7 & 0 & -T_8 & 0 & 0 & 0 & -T_9 \\
0 & 0 & 0 & -T_{10} & 0 & -T_{11} & 0 & 0 & 0 & -T_{12} \\
0 & 0 & 0 & 0 & -x_6 & 0 & 0 & 0 & 0 & 0 \\
0 & 0 & 0 & 0 & 0 & -x_8 & 0 & 0 & 0 & 0 \\
0 & 0 & 0 & 0 & 0 & 0 & -x_9 & 0 & 0 & 0 \\
0 & 0 & 0 & 0 & 0 & 0 & 0 & -x_{11} & 0 & 0 \\
0 & 0 & 0 & 0 & 0 & 0 & 0 & 0 & -x_{13} & 0 \\
0 & 0 & 0 & 0 & 0 & 0 & 0 & 0 & 0 & -x_{14}
\end{pmatrix} \tag{22}$$

Where:

$$T_1=\frac{\ell\varphi-x_1x_3}{x_1},\ T_6=\frac{\ell\varphi x_4+\varepsilon_1\nu_1x_3-x_1x_3x_4}{\ell\varphi-x_1x_3}\ \text{and}$$

$$T_{10}=\frac{\ell\varphi x_4x_5+\varepsilon_1\nu_1x_3x_5+\varepsilon_2\nu_1\nu_2x_3-x_1x_3x_4x_5}{\ell\varphi x_4+\varepsilon_1\nu_1x_3-x_1x_3x_4}$$

Then, the characteristics polynomial of matrix (22) is given as

$$\begin{pmatrix}
-x_1-n & \ell & \varepsilon_1 & \varepsilon_2 & 0 & x_2 & 0 & 0 & 0 & \eta \\
0 & -T_1-n & T_2 & T_3 & 0 & T_4 & 0 & 0 & 0 & T_5 \\
0 & 0 & -T_6-n & -T_7 & 0 & -T_8 & 0 & 0 & 0 & -T_9 \\
0 & 0 & 0 & -T_{10}-n & 0 & -T_{11} & 0 & 0 & 0 & -T_{12} \\
0 & 0 & 0 & 0 & -x_6-n & 0 & 0 & 0 & 0 & 0 \\
0 & 0 & 0 & 0 & 0 & -x_8-n & 0 & 0 & 0 & 0 \\
0 & 0 & 0 & 0 & 0 & 0 & -x_9-n & 0 & 0 & 0 \\
0 & 0 & 0 & 0 & 0 & 0 & 0 & -x_{11}-n & 0 & 0 \\
0 & 0 & 0 & 0 & 0 & 0 & 0 & 0 & -x_{13}-n & 0 \\
0 & 0 & 0 & 0 & 0 & 0 & 0 & 0 & 0 & -x_{14}-n
\end{pmatrix} \tag{23}$$

Now, taking the product of the diagonal elements of matrix (23) gives the eigenvalues as:

$$n_1 = -(v_1+\varphi+\mu),\ n_2 = -\frac{\ell\varphi+(v_1+\varphi+\mu)(\ell+\mu)}{v_1+\varphi+\mu},\ n_5 = -(\sigma+\mu+\theta),\ \ n_6 = -(\xi+\mu)$$

$$n_7 = -(\lambda+\mu),\ \ n_8 = -(\gamma+\mu+\delta),\ n_9 = -(\tau+\mu+\delta)\left(-T_6-n_3\right),\ \ n_{10} = -(\gamma+\mu)$$

$$n_3 = -\frac{\ell\varphi(v_2+\varepsilon_1+\mu)+\varepsilon_1 v_1(\ell+\mu)-(v_1+\varphi+\mu)(\ell+\mu)(v_2+\varepsilon_1+\mu)}{\ell\varphi-(v_1+\varphi+\mu)(\ell+\mu)}$$

$$n_4 = -\frac{\ell\varphi(v_2+\varepsilon_1+\mu)(\varepsilon_2+\mu)+\varepsilon_1 v_1(\ell+\mu)(\varepsilon_2+\mu)+\varepsilon_2 v_1 v_2(\ell+\mu)-(v_1+\varphi+\mu)(\ell+\mu)(v_2+\varepsilon_1+\mu)(\varepsilon_2+\mu)}{\ell\varphi(v_2+\varepsilon_1+\mu)+\varepsilon_1 v_1(\ell+\mu)-(v_1+\varphi+\mu)(\ell+\mu)(v_2+\varepsilon_1+\mu)} \tag{24}$$

From equation (24), $n_1, n_2, n_3, n_4, n_5, n_6, n_7, n_8, n_9, n_{10} < 0,$ which proves theorem 2 as required. Thus, the disease-free equilibrium point is locally asymptotically stable.

3.7 Global stability of disease-free equilibrium point

We used Castillo-Chavez theorem Castillo-Chavez *et al*. (2002) to investigate the global asymptotic stability of the disease-free state. For the theorem to work, we rewrite (2) in the form:

$$\frac{dX}{dt} = H(X,Z)$$
$$\frac{dZ}{dt} = G(X,Z), G(X,0) = 0 \tag{25}$$

where $X = (S, N_p, V_1, V_2, R)$ and $Z = (E, Q, A, I, H,)^T$. Here, the components of $X \in \mathbb{R}^5$ denote the uninfected individuals and the components of $Z \in \mathbb{R}^5$ denote the infected individuals. The disease-free equilibrium of the system now becomes $E_0^* = (X^*, 0)$. To guarantee global asymptotic stability, the following two conditions must be met.

i. $\frac{dX}{dt} = H(X,0),\ X^*$ is globally asymptotically stable (GAS)

ii. $G(X,Z) = PZ - \hat{G}(X,Z),\ \hat{G}(X,Z) \geq 0$ for $(X,Z) \in \Omega$

where $P = D_Z G(X^*, 0)$ is an M matrix (the off diagonal elements of P are non-negative) and Ω is the region where the model is biologically meaningful. If the system satisfies conditions (i) and (ii) then the following theorem holds.

Theorem 3: The fixed point $E_0^* = (X^*, 0)$ is a globally asymptotic stable equilibrium provided that $R_0 < 1$ and the assumptions (i) and (ii) are satisfied.

Proof.

Since $X = (S, N_p, V_1, V_2, R)$ and $Z = (E, Q, A, I, H,)^T$ then

Then,

$$H(X,0) = \begin{bmatrix} (1-\rho)\Pi + \ell N_p + \varepsilon_1\upsilon_1 + \varepsilon_2\upsilon_2 - (\upsilon_1+\varphi+\mu)S \\ \varphi S - (\ell+\mu)N_p \\ v_1 S - (v_2+\varepsilon_1+\mu)V_1 \\ \rho\Pi + v_2 V_1 - (\varepsilon_2+\mu)V_2 \\ 0 \end{bmatrix} \tag{26}$$

and

$$\hat{G}(X,Z) = PZ - G(X,Z)$$

Where:

$$G(X,Z) = \begin{bmatrix} \beta_S S + \beta_s(1-\in)V_1 - (\sigma+\mu+\theta)E \\ \theta E - (\xi+\mu)Q \\ \sigma(1-\psi)E - (\lambda+\mu)A \\ \sigma\psi E + \lambda(1-\phi)A - (\gamma+\mu+\delta)I \\ \xi\alpha Q + \gamma(1-\kappa)I - (\tau+\mu+\delta)H \end{bmatrix} \tag{27}$$

and $P = D_Z G(X^*, 0)$ is the Jacobian of $G(X,Z)$ with respect to Z, such that

$$P = \begin{bmatrix} -(\sigma+\mu+\theta) & 0 & \frac{\omega_A}{N}S^* + \frac{\omega_A}{N}(1-\in)V_1^* & \frac{\omega_I}{N}S^* + \frac{\omega_I}{N}(1-\in)V_1^* & \frac{\omega_H}{N}S^* + \frac{\omega_H}{N}(1-\in)V_1^* \\ \theta & -(\xi+\mu) & 0 & 0 & 0 \\ \sigma(1-\psi) & 0 & -(\lambda+\mu) & 0 & 0 \\ \sigma\psi & 0 & \lambda(1-\phi) & -(\gamma+\mu+\delta) & 0 \\ 0 & \xi\alpha & 0 & \gamma(1-\kappa) & -(\tau+\mu+\delta) \end{bmatrix} \tag{28}$$

Then,

$$PZ - G(X,Z) = \hat{G}(X,Z)$$

$$= \begin{bmatrix} \beta_s\left(\frac{(\nu_2+\varepsilon_1+\mu)(\ell+\mu)\Pi\left((\varepsilon_2+\mu)(1-\rho)+\varepsilon_2\rho\right)}{(\nu_2+\varepsilon_1+\mu)(\varepsilon_2+\mu)\left((\nu_1+\varphi+\mu)(\ell+\mu)-\ell\varphi\right)-(\ell+\mu)\left((\varepsilon_2+\mu)\varepsilon_1\nu_1+\varepsilon_1\nu_1\nu_2\right)} - S\right) \\ 0 \\ 0 \\ 0 \\ 0 \end{bmatrix} \tag{29}$$

With $\dfrac{(\nu_2+\varepsilon_1+\mu)(\ell+\mu)\Pi\left((\varepsilon_2+\mu)(1-\rho)+\varepsilon_2\rho\right)}{(\nu_2+\varepsilon_1+\mu)(\varepsilon_2+\mu)\left((\nu_1+\varphi+\mu)(\ell+\mu)-\ell\varphi\right)-(\ell+\mu)\left((\varepsilon_2+\mu)\varepsilon_1\nu_1+\varepsilon_1\nu_1\nu_2\right)} \geq S$

Which implies that $\hat{G}(X,Z) \geq 0$. Therefore, the conditions (i) and (ii) have been met and hence E_0^* is Globally Asymptotically Stable (GAS).

4. Numerical Simulations

To illustrate the theoretical results, numerical simulations are carried out. Model parameter values for the numerical simulations with their description and source are listed in Table 1. Whenever parameter values were not available in the literature, we assumed realistic values for the purpose of illustration.

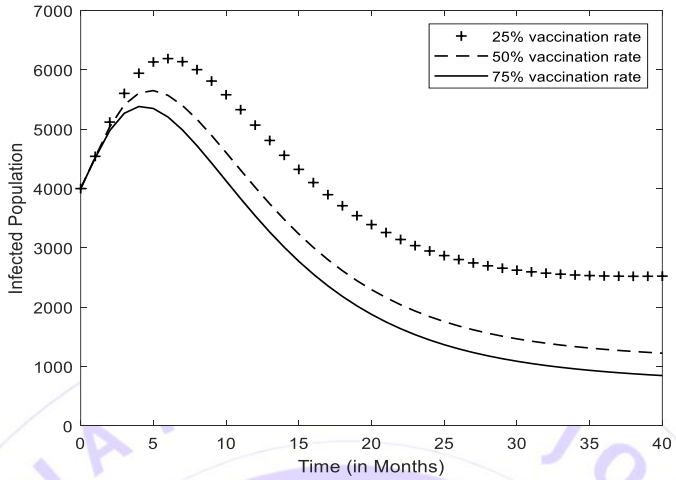

Figure 2: Impact of first and second dose of COVID-19 vaccine only on infected population at different rate (i.e V_1 =0.25, 0.50, 0.75 with V_2 fixed at 0.8).

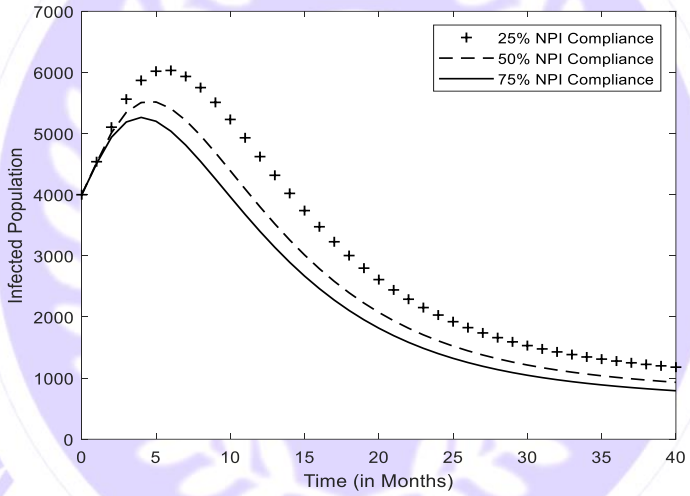

Figure 3: Impact of Non-pharmaceutical intervention only on infected population at different rate of NPI compliance (i.e φ =0.25, 0.50, 0.75)

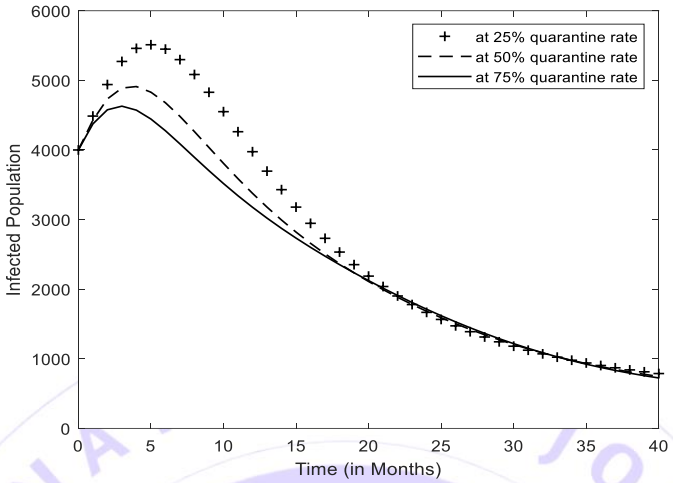

Figure 4: Impact of contact tracing and quarantine only on the infected population at different rate of quarantine (i.e θ =0.25, 0.50, 0.75).

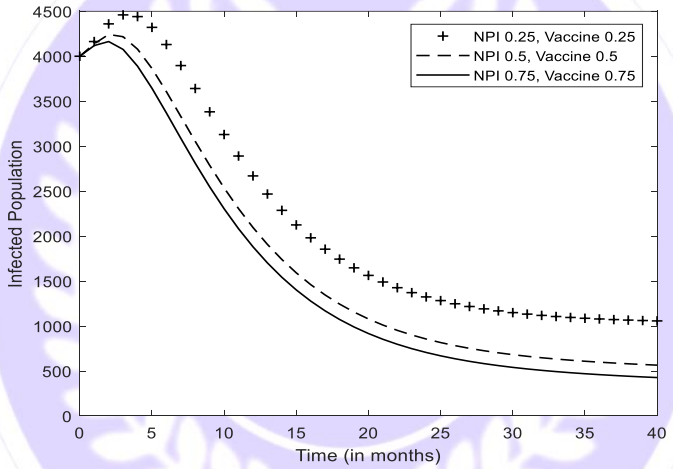

Figure 5: Impact of non-pharmaceutical and COVID-19 vaccine only on the infected population at different rate (i.e $\varphi = \nu_1$ =0.25, 0.50, 0.75 with ν_2 fixed at 0.8)

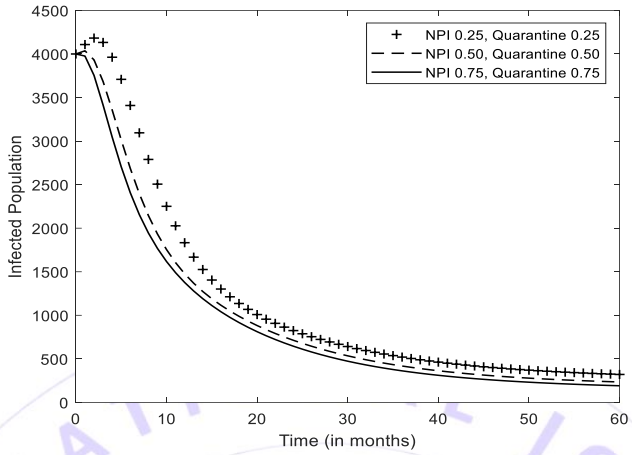

Figure 6: Impact of non-pharmaceutical intervention and quarantine only on the infected individuals at different rates (i.e $\varphi = \theta$ =0.25, 0.50, 0.75).

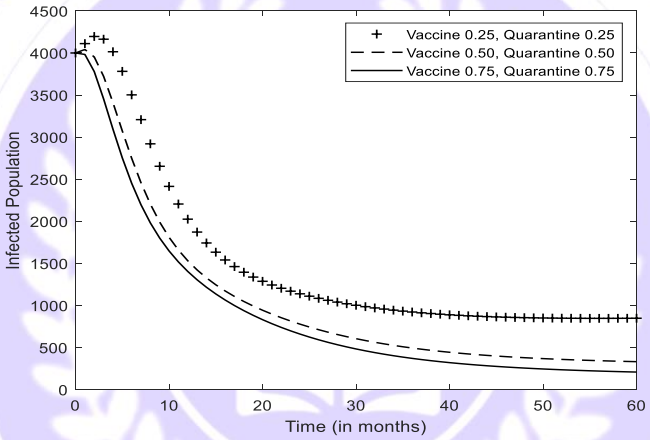

Figure 7: Impact of COVID-19 vaccine and quarantine only on the infected individuals at different rates (i.e $v_1 = \theta$ =0.25, 0.50, 0.75 with V_2 fixed at 0.8).

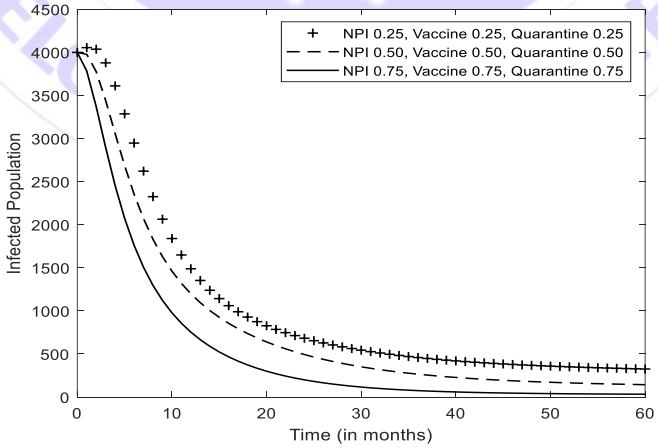

Figure 8: Impact of all the control strategies (non-pharmaceutical intervention, COVID-19 vaccine and quarantine) on the infected individuals at different rates (i.e $\varphi = v_1 = \theta$ =0.25, 0.50, 0.75 with V_2 fixed at 0.8).

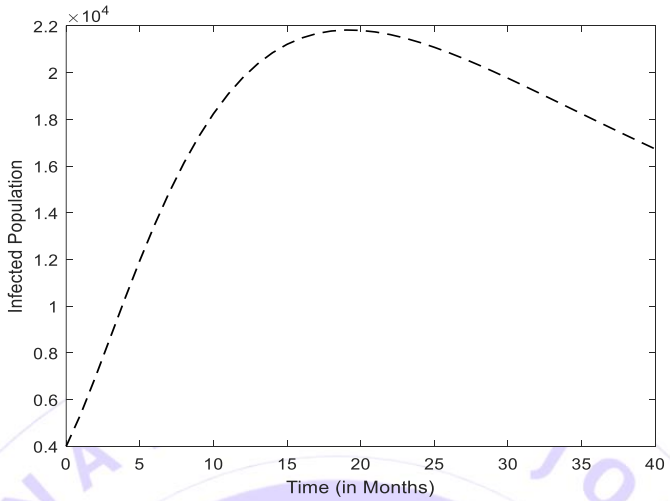

Figure 9: Simulation result of infectious human population without any intervention ($\varphi = \theta = v_1 = v_2 = 0$)

5. Discussion

Figure 2 shows the impact of COVID-19 vaccine (first and second doses) on the dynamics of infectious human population at different vaccination rates. The population of the infectious humans decreases slowly as vaccination rates increase. When the vaccination rate is 0.25 with a basic reproduction number $(R_0 = 0.7865)$, the infectious human population rises to 6,000 before decreasing to 2,500. At a 0.50 vaccination rate, with a basic reproduction number $(R_0 = 0.4433)$, the infectious human population was reduced to 1,200. While at 0.75 vaccination rate, with a basic reproduction number $(R_0 = 0.3186)$, the infectious human population reduced to 850. Therefore, the simulation indicates that first and second dose of vaccination plays a vital role in the reducing the spread of COVID-19 disease.

Figure 3 shows the impact of non-pharmaceutical intervention strategies on the infectious human population. From our simulation result, we can see that the infectious human population is decreasing when the rate of NPIs is increasing. At a 0.25 rate of compliance with NPIs with the basic reproduction number $(R_0 = 0.2353)$, the infectious human population was reduced to 1,150. At a 0.50 NPIs compliance rate, with a basic reproduction number $(R_0 = 0.1200)$, the infectious human population was reduced to 980. While at 0.75 NPIs compliance rate with basic reproduction number $(R_0 = 0.0855)$, the infectious human population reduced to 850. As we can see, both the simulation and analytical results indicate that compliance with the non-pharmaceutical intervention strategy is more effective than the vaccine in curtailing the spread of COVID-19.

We further analyzed the impact of quarantine at different rates on the dynamics of infectious human population in Figure 4. The infectious human population was reduced below 1,000 at all the quarantine rates used. At a 0.25 quarantine rate with a basic reproduction number $(R_0 = 0.9254)$, the infectious human population rise to 5,800 before decreasing to 900. While at 0.5 and 0.75 quarantine rates with basic reproduction numbers $(R_0 = 0.8747)$ and $(R_0 = 0.6132)$ respectively, the infectious human population rise to 4,900 and 4,500 respectively, before decreasing to 850. Therefore, both the simulation and analytical results indicate that vaccination and non-pharmaceutical intervention strategies are more effective in curtailing the spread of COVID-19 compared to quarantine.

Furthermore, figures (5) to (8) show the combination of two intervention strategies, i.e., NPIs with vaccine, NPIs with quarantine, and vaccine with quarantine. All the experiments show a great reduction in the infectious human population. In Figure 4, which is the combination of NPIs with vaccines, the infectious human population rise to 4500 before decreasing to 1,200 at 0.25 NPIs and vaccination rates with the basic reproduction number $(R_0 = 0.1953)$. When the NPIs and vaccination rates are 0.5 with basic reproduction number $(R_0 = 0.1048)$, the infectious human population reduced to 600 while when the NPIs and vaccination rate are 0.75 with basic reproduction number $(R_0 = 0.0741)$, the infectious human population was reduced to 400.

Figure (6) shows the impact of NPIs and quarantine on the infectious human population. From the simulation, we can

see that the infectious human population rose to 4,200 before decreasing to 300 in 60 months at 0.25 NPIs and a quarantine rate with a basic reproduction number $(R_0 = 0.0603)$. At 0.5 NPIs and a quarantine rate with a basic reproduction number $(R_0 = 0.0307)$, the infected human population was reduced to 200. While at 0.75 NPIs and quarantine rate with a basic reproduction number $(R_0 = 0.0083)$, the infected human population reduced to 150.

In Figure 7, the infected human population rises to 4,300 before decreasing to 850 in 60 months when the rate of vaccination and quarantine is 0.25 with the basic reproduction number $(R_0 = 0.2015)$. At a 0.5 vaccination and quarantine rates with a basic reproduction number $(R_0 = 0.0651)$, the infected human population is reduced to 350, while it is reduced to 250 when the vaccine and quarantine rate is 0.75 with basic reproduction number $(R_0 = 0.0328)$. Therefore, both the simulation and analytical results indicate that the combination of non-pharmaceutical intervention with quarantine as control strategy is more effective than the other two combinations (i.e non-pharmaceutical intervention with vaccine and quarantine with vaccine) in curtailing the spread of COVID-19.

We have also analyzed the impact of vaccination, non-pharmaceutical intervention and quarantine at different rates on the infected human population as shown in figure 8. The implementation of both vaccination, non-pharmaceutical intervention and quarantine is very effective and has reduced the number of infected individuals significantly. At 0.25 vaccination, NPIs and quarantine rates with the basic reproduction number $(R_0 = 0.0500)$, the infected human population was reduced to 300. When the vaccination, NPIs and quarantine rate is 0.5 with a basic reproduction number $(R_0 = 0.0154)$, the infected human population is reduced to 150, and the population is almost getting to 0 when the rate of vaccine, NPIs and quarantine is 0.75 with the basic reproduction number $(R_0 = 0.0076)$.

Finally, the numerical result in experiment eight, depicted in figure 9, shows the absence of COVID-19 vaccine, non-pharmaceutical intervention and quarantine. More than half of the population has started showing symptoms of COVID-19 (symptomatic individuals increased to 22,000), and the analytical result also shows the basic reproduction number is greater than unity $(R_0 = 5.9544)$. The epidemiological implementation of the result is that the transmission of COVID-19 can be significantly curtailed with a basic reproduction number less than unity ($R_0 < 0$), which implies that vaccination, non-pharmaceutical intervention and quarantine can lead to effective control or elimination of the disease.

6. Conclusion

Based on the findings of this study, it has been established that the COVID-19 pandemic can be effectively controlled or eradicated by the use of vaccine, non-pharmaceutical interventions, contact tracing, and quarantine. Therefore, we hereby recommend that the relevant agencies devise a strategy to educate the public about the necessity of getting vaccinated against COVID-19 in order to protect themselves from infection. Adequate and effective vaccination implementation, along with non-pharmaceutical interventions, are necessary in order to completely prevent or curtail COVID-19 infection.

References

Babaei, A., Jafari, H., Banihashemi, S. and Ahmadi, M. (2021). Mathematical analysis of a stochastic model for spread of Coronavirus. *Chaos, Solitons and Fractals*, vol. 145, article 110788. doi: 10.1016/j.chaos.2021.110788.

Brauer, F., van den Driessche, P. and Jianhong, W. (2020). Lecture Notes in Mathematical Epidemiology, Compartmental Models in Epidemiology: Chapter 2, Department of Mathematics, University of British Columbia -Springer-Verlag.

Bubar, K. M., Reinholt, K., and Kissler, S. M. (2021). Model-informed COVID-19 vaccine prioritization strategies by age and serostatus. *Science*, vol. 371, no. 6532, pp. 916–921. doi: 10.1126/science.abe6959.

Castillo-Chavez, C., Feng, Z. and Huang, W. (2002). On the computation of R_0 and its Role in Global Stability," *IMA Volumes in Mathematics and Its Applications*, vol. 125, pp. 229–250.

Diagne, M. L., Rwezaura, H., Tchoumi, S. Y. and Tchuenche, J. M. (2021). A Mathematical Model of COVID-19 with Vaccination and Treatment. *Journal of Computational and Mathematical Methods in Medicine*. Vol. 2021, Pp 16. https://doi.org/10.1155/2021/1250129.

Eric N. W., Ernest D. A., and Daniel E. B. (2020). Modelling the Dynamics of COVID-19 Disease with Contact Tracing and Isolation in Ghana. *Mathematical Modelling and Applications.* Vol. 5, No. 3, 2020, pp. 146-155. doi: 10.11648/j.mma.20200503.13.

Feng L. X., Jing S. L., Hu S. K., Wang D. F., and Huo H. F. (2020). Modelling the Effects of Media Coverage and Quarantine on the COVID-19 Infections in the UK. *Mathematical Biosciences and Engineering*, vol. 17, no. 4, pp. 3618–3636.

Harvard Medical School (2020). Treatments for COVID-19: What helps, What doesn't, and What's in the Pipeline. Harvard Health Publishing. Retrieved on 14th July 2020, health.harvard.edu/diseasesand-conditions/treatments-for-covid-19.

Iboi, E. A., Sharomi, O., Ngonghala, C. N., & Gumel A. B. (2020). Mathematical modelling and analysis of COVID-19 Pandemic in Nigeria. *Mathematical Biosciences and Engineering*, 17(6), Pp. 7192-7220. https://doi.org/10.3934/MBE.2020369.

Ibrahim, O. M. and Ekundayo, D. D. (2020). COVID-19 Pandemic in Nigeria: Misconception among Individuals, Impact on Animal and the Role of Mathematical Epidemiologists. Preprints, 2020040492, 2020. DOI: 10.20944/preprints202004.0492.

Imai, N., Cori, A., Dorigatti, I., Beguelin, M., Donnelly, A., Riley, S. and Ferguson, N. (2020). Report 3: Transmissibility of 2019-nCoV. *Imperial College London COVID-19 Response Team.* https://doi.org/10.25561/77148.

Madubueze, C. E., Dachollom, S. and Onwubuya, I. O. (2020). Controlling the Spread of COVID-19: Optimal Control Analysis. *Computational and Mathematical Methods in Medicine*, vol. 2020, no. 6862516. https://doi.org/10.1155/2020/6862516.

Ministry of Health, Ghana. (2019). COVID-19 Ghana's Outbreak Response Management Update. https://ghanahealthservice.org/covid19.

NCDC. (2020). COVID-19 Situation Report. Situation Report 1, 2020. Retrieve on 07/07/2020 from https://ncdc.gov.ng/disease/sitreps/?cat=14andname=An.

Okuonghae, D. and Omame, A. (2020). Analysis of a Mathematical Model for COVID-19 Population Dynamics in Lagos, Nigeria. *Chaos, Solitons and Fractals*, 139: 110032. https://doi.org/10.1016/j.chaos.2020.110032.

Pedro, S. A., Ndjomatchoua, F. T., Jentsch, P., Tchuenche, J. M., Anand, M. and Bauch, C. T. (2020). Conditions for a Second Wave of COVID-19 Due to Interactions Between Disease Dynamics and Social Processes. *Frontiers of Physics*, vol. 8, article 574514. doi: 10.3389/fphy.2020.574514.

Prieto, C. R. and González R. H. (2021). Vaccination Strategies Against COVID-19 and the Diffusion of Anti-Vaccination Views. *Scientific Reports*, vol. 11, no. 1, p. 6626. https://doi.0rg/10.1038/s41598-021-85555-1.

Safi, M. A. and Gumel, A. B. (2011). Mathematical Analysis of a Disease Transmission Model with Quarantine, Isolation and An Imperfect Vaccine. *Computers and Mathematics with Applications*, 61: 3044–3070. https://doi.org/10.1016/j.camwa.2011.03.095.

World Health Organization (2019). Malaria and COVID-19, 2019, December 2019. https://www.who.int/teams/global-malaria-programme/covid-19.

World Health Organization (2020). Coronavirus Disease 2019 (COVID-19). *Situation Report -51*, Data as reported by 11 March, 2020. Retrieve on 24/04/2020 from http://www.who.int/emergencies/disease/novel-coronavirus-2019/situation-reports.

Wu, J. T., Leung, K. and Leung, G. M. (2020). Nowcasting and Forecasting the Potential Domestic and International

Spread of the 2019-nCoV Outbreak Originating in Wuhan, China: A Modelling Study. *The Lancet*, vol. 395, no. 10225, Pp. 689–697. https://doi.org/10.1016/S0140-6736(20)30260-9.